Available online at www.sciencedirect.com

SCIENCE DIRECT®

Journal of Computational and Applied Mathematics 192 (2006) 40–50

JOURNAL OF COMPUTATIONAL AND APPLIED MATHEMATICS

www.elsevier.com/locate/cam

Numerical analysis of pressure field on curved self-weighted metallic roofs due to the wind effect by the finite element method

J.J. del Coz Díaz[a,*], P.J. García Nieto[b], F.J. Suárez Domínguez[a]

[a] *Department of Construction, University of Oviedo, Edificio Dep. de Viesques no 7, 33204, Spain*
[b] *Department of Mathematics, University of Oviedo, Facultad de Ciencias, 33007, Spain*

Received 15 September 2004; received in revised form 15 February 2005

Abstract

In this paper, an evaluation of distribution of the air pressure is determined throughout the curved and open self-weighted metallic roof due to the wind effect by the finite element method (FEM) [K. Bathe, Finite Element Procedures, Prentice-Hall, Englewood Cliffs, New York, 1996]. Data from experimental tests carried out in a wind tunnel involving a reduced scale model of a roof was used for comparison. The nonlinearity is due to time-averaged Navier–Stokes equations [C.A.J. Fletcher, Computational Techniques for Fluid Dynamics, Springer, Berlin, 1991] that govern the turbulent flow. The calculation has been carried out keeping in mind the possibility of turbulent flow in the vicinities of the walls, and speeds of wind have been analyzed between 30 and 40 m/s. Finally, the forces and moments are determined on the cover, as well as the distribution of pressures on the same one, comparing the results obtained with the Spanish and European Standards rules, giving place to the conclusions that are exposed in the study.

MSC: 74S05; 35Q30

Keywords: Computational fluid dynamics; Finite element modeling; Numerical and experimental methods; k–ε model; Steady incompressible flow; Curved self-weighted metallic roofs

* Corresponding author. Tel.: +34 985 18 20 42; fax: +34 985 18 24 33.
E-mail address: juanjo@constru.uniovi.es (J.J. del Coz Díaz).

0377-0427/$ - see front matter © 2005 Elsevier B.V. All rights reserved.
doi:10.1016/j.cam.2005.04.035

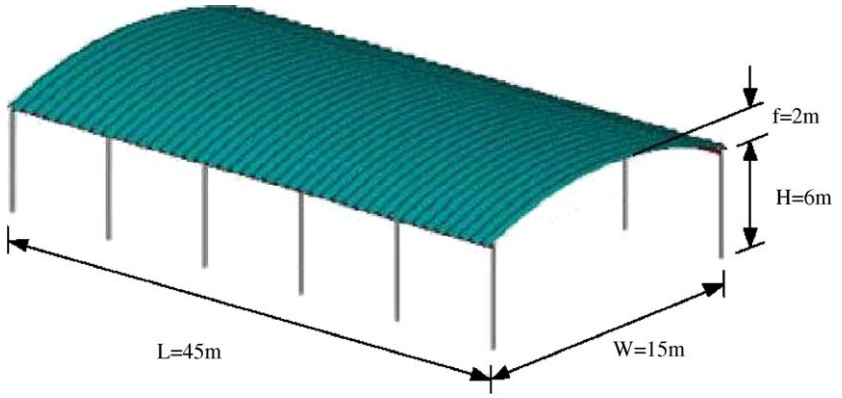

Fig. 1. Dimensions of the roof.

1. Introduction

The finite element method is a numerical procedure than can be used to obtain solutions to a large class of engineering problems involving stress analysis, heat transfer, electromagnetism, and in our case 'fluid flow' [1,2,4]. This work was written to help one gain a clear understanding of the basic concepts which will enable one to use a general-purpose finite element software, such as ANSYS [6] effectively to calculate the pressure field on curved self-weighted metallic roofs due to the wind effect.

In general, engineering problems are mathematical models of physical situations. Mathematical models are differential equations with a set of corresponding boundary and initial conditions. The differential equations are derived by applying the fundamental laws and principles of nature to a system or a control volume. These governing equations represent balance of mass, force, or energy [3].

In any given engineering problem, there are two sets of parameters that influence the way in which a system behaves. First, there are those parameters that provide information regarding the 'natural behavior' of a given system. These parameters include properties such as viscosity, and thermal conductivity [5].

On the other hand, there are parameters that produce 'disturbances' in a system. Examples of these parameters include external forces, moments, and pressure difference in fluid flow [5]. It is important to understand the role of these parameters in finite element modeling in terms of their respective appearances in stiffness or conductance matrices and load or forcing matrices. The system characteristics will always show up in the stiffness matrix, whereas the disturbance parameters will always appear in the load matrix. In order to solve this nonlinear problem, we have to choose the appropriate finite element as well as the suitable geometry.

The system of self-weighted roofs constitutes an original alternative in the construction field (see Fig. 1). The Blocotelha/Intertelha shells carry out a double function based on the principle that the element of roof has to work like resistant element too: on the one hand they act like beam and on the other hand like casing.

The use of finite element method [10] shows innumerable advantages of economical and practical order due, on the one hand, to the cost that plays the realization of real tests, and in the other hand, to the technical difficulty of the same, since the elements object of the present study are big in size. The main objective of this paper is to determine, by the finite element method [1], the distribution of the

air pressure throughout the curved and open self-weighted metallic roof on which a strong wind falls horizontally.

In order to carry out this work, the program FLOTRAN of the application ANSYS version 5.7 has been used [6]. This program for the analysis by the finite element method developed for personal computers and work stations by Swanson Analysis Systems Inc. (SASI) is one of the most universally used and known. In the model, the air is divided into tridimensional finite elements of eight nodes, of this kind incompressible fluid with the characteristic properties of air. The finite element chosen is FLUID 142 [6].

Following are the dimensions of the roof as indicated in Fig. 1: length: $L = 45\,\text{m}$; width: $W = 15\,\text{m}$; height: $H = 6\,\text{m}$; arrow: $f = 2\,\text{m}$; and curvature radius: $R = 15\,\text{m}$.

On the other hand, the company Blocotelha orders a report with the results given by test carried out in a wind tunnel [8]. The test was performed on a reduced scale model (1:100) of a roof with dimensions like the above described.

2. Geometry

2.1. Domain of the finite element model

It is understood for domain that all the space points where the objective functions must verify the differential equations of the model. In a boundary value problem, the values of some degrees of freedom in the boundary of domain are known.

For this problem of external flow around a body, the domain is an air volume that contains the roof. This air box is divided into finite elements with the characteristic properties of the air. This process is called meshing. All the volume of the box is meshed excepting but the space occupied (taken) by the roof.

The size of the air box in the models, where the flow is studied around the body, is submerged in a stream. The position of the body inside the domain depends on the size and shape of the body, as well as the fluid-dynamical characteristics of the problem.

The appearance which the geometry of the finite element model will have, is shown in Fig. 2, an air volume in the interior of which the roof is found.

3. Characterization of the air flow

3.1. Turbulent regime

The difference between the laminar regime and the turbulent regime lies in the relative magnitude of the inertial forces and the viscosity forces. By low velocities the motion of fluid is smooth and orderly. By higher velocities the transition is started and turbulent eddies appear. By high velocities the flow fluctuates permanently and it is considered turbulent. In order to measure quantitatively the degree of turbulence, the dimensionless Reynolds number is used [5]:

$$Re = \frac{\rho V L}{\mu} = \frac{V L}{\nu}, \tag{1}$$

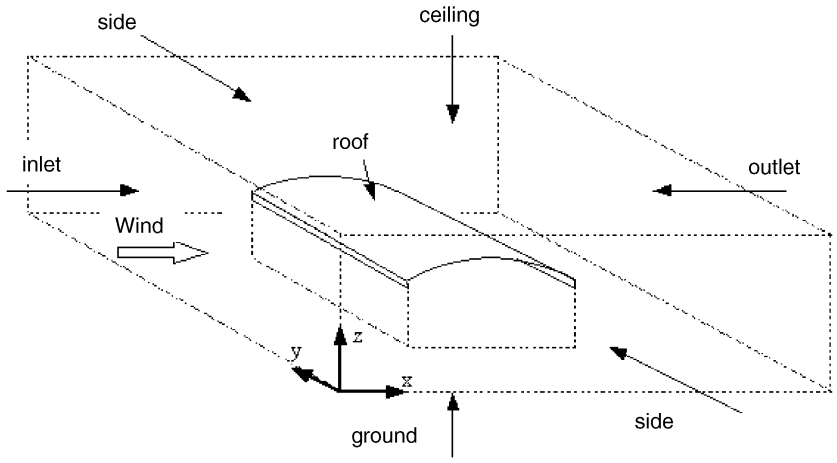

Fig. 2. Geometry of the finite element model.

where ρ is the density of fluid, V the velocity of nondisturbed stream, L the characteristic length, μ the dynamic viscosity of fluid, and ν the kinematic viscosity of the fluid ($\nu = \mu/\rho$).

In a flat or quasi-flat body submerged in an air stream, for example the wing of an airplane, the characteristic length is the cord or length of the body parallel to the stream. In case of the self-weighted roof with cross wind, for a velocity of stream of 30 m/s (= 110 km/h) and for width of the roof of 15 m, the value of Reynolds number is:

$$Re = \frac{1.205\,\mathrm{kg/m^3}\,30\,\mathrm{m/s}\,15\,\mathrm{m}}{1.8\cdot 10^{-5}\,\mathrm{kg/m\cdot s}} = 3\cdot 10^7. \tag{2}$$

This value is high enough to consider the turbulent regime.

3.2. Turbulence averaged quantities

For any quantity A the separation:

$$A = \bar{A} + A', \tag{3}$$

$$\bar{A}(\vec{x}, t) = \frac{1}{T}\int_{-T/2}^{T/2} A(\vec{x}, t+\tau)\,\mathrm{d}\tau, \tag{4}$$

where T is to be chosen large enough compared with the same time scale of the turbulence but still small compared with those of all other unsteady phenomena.

Obviously, this might not be always possible: if unsteady phenomena occur with time scales of the same order as those of the turbulent fluctuations the Reynolds-averaged equations will not allow us to model these phenomena.

However, it can be considered that most of the unsteady phenomena in fluid dynamics have frequency ranges outside the frequency range of turbulence [2].

For compressible flows the averaging process leads to products of fluctuations between density and the other variables such as velocity or internal energy. In order to avoid their explicit occurrence a density-weighted average can be introduced, through

$$\tilde{A} = \frac{\overline{\rho A}}{\bar{\rho}} \tag{5}$$

with

$$A = \tilde{A} + A'' \tag{6}$$

and

$$\overline{\rho A''} = 0. \tag{7}$$

This way of defining mean turbulent variables will remove all additional products of density fluctuations with other fluctuating quantities. This is easily seen by performing the averaging process defined by Eq. (5) on the continuity equation, leading to:

$$\frac{\partial}{\partial t}\bar{\rho} + \vec{\nabla} \cdot (\bar{\rho}\tilde{\vec{v}}) = 0. \tag{8}$$

A more complete discussion can be found in [5,7]. Applied to the momentum equations, the following equation for the turbulent mean momentum is obtained, in the absence of body forces:

$$\frac{\partial}{\partial t}(\bar{\rho}\tilde{\vec{v}}) + \vec{\nabla} \cdot (\bar{\rho}\tilde{\vec{v}} \otimes \tilde{\vec{v}} + \bar{p}\bar{\bar{I}} - \bar{\bar{\tau}}^{v} - \bar{\bar{\tau}}^{R}) = 0, \tag{9}$$

where the Reynolds stresses, $\bar{\bar{\tau}}^{R}$, defined by:

$$\bar{\bar{\tau}}^{R} = \overline{-\rho\vec{v}'' \otimes \vec{v}''} \tag{10}$$

are added to the averaged viscous shear stresses $\bar{\bar{\tau}}^{V}$. In Cartesian coordinates we have

$$\tau_{ij}^{R} = \overline{-\rho v_i'' v_j''}. \tag{11}$$

The relations between the Reynolds stresses and the mean flow quantities are unknown. Therefore the application of the Reynolds-averaged equations to the computation of turbulent flows requires the introduction of some modeling of these unknown relations, based on theoretical considerations coupled with unavoidable empirical information. In a similar way, the turbulent averaged energy conservation equation can be obtained under different forms according to the definition taken for the averaged total energy.

3.3. The Reynolds-averaged Navier–Stokes equations

The turbulent averaging process is introduced in order to obtain the laws of motion for the 'mean', time-averaged, turbulent quantities [2,4]. This time averaging is to be defined in such a way as to remove the influence of the turbulent fluctuations while not destroying the time dependence associated with other time-dependent phenomena with time scales distinct from those of turbulence.

3.4. Turbulent flow

For incompressible flows that are turbulent, the use of the three-dimensional equivalent of Navier–Stokes equations would be too expensive for engineering design calculations. For most practical calculations, the mean motion is of primary interest. This can be obtained by first averaging the equations over a small time T. This process produces the time-averaged governing equations [2]:

$$\frac{\partial \bar{u}}{\partial x} + \frac{\partial \bar{v}}{\partial y} = 0, \tag{12}$$

$$\rho\left(\frac{\partial \bar{u}}{\partial t} + \bar{u}\frac{\partial \bar{u}}{\partial x} + \bar{v}\frac{\partial \bar{u}}{\partial y}\right) + \frac{\partial \bar{p}}{\partial x} = \frac{\partial}{\partial x}\left(\mu\frac{\partial \bar{u}}{\partial x} - \overline{\rho u'u'}\right) + \frac{\partial}{\partial y}\left(\mu\frac{\partial \bar{u}}{\partial y} - \overline{\rho u'v'}\right), \tag{13}$$

$$\rho\left(\frac{\partial \bar{v}}{\partial t} + \bar{u}\frac{\partial \bar{v}}{\partial x} + \bar{v}\frac{\partial \bar{v}}{\partial y}\right) + \frac{\partial \bar{p}}{\partial y} = \frac{\partial}{\partial x}\left(\mu\frac{\partial \bar{v}}{\partial x} - \overline{\rho u'v'}\right) + \frac{\partial}{\partial y}\left(\mu\frac{\partial \bar{v}}{\partial y} - \overline{\rho v'v'}\right), \tag{14}$$

where $\bar{u}$, $\bar{v}$ are turbulent fluctuations and u', v' are turbulent fluctuations. For three-dimensional flows additional Reynolds stress $-\overline{\rho u'w'} - \overline{\rho v'w'} - \overline{\rho w'w'}$ appear in the equivalent of (13) and (14). The time-averaged equations can be solved if the Reynolds stresses can be related to mean flow quantities. This is done by introducing an eddy viscosity ν_T, letting $-\overline{\rho u'v'} = \rho\nu_T \partial u/\partial y$, and introducing algebraic formulae for the eddy viscosity ν_T, etc. However, although this is effective for boundary layer flow, where the local production of turbulent energy is approximately equal to the rate of dissipation, it may not be effective for more complicated turbulent flows, where the transport of turbulence quantities is also important. An alternative approach is to construct (differential) transport equations for some of the turbulence quantities and to model higher-order terms, which turn out to be triple correlations. Here, we indicate the form of a typical two-equation turbulence model, the k–ε model [2]. In the k–ε model differential equations are introduced for the turbulent kinetic energy k and the rate of dissipation of turbulent energy ε [7,9], where

$$k = 0.5(\overline{u'u'} + \overline{v'v'} + \overline{w'w'}) = 0.5(\overline{u_i'u_i'}) \tag{15}$$

and

$$\varepsilon = \nu_T\overline{\left(\frac{\partial u_i'}{\partial x_j}\right)\left(\frac{\partial u_i'}{\partial x_j}\right)}. \tag{16}$$

Because of the complexity of the equations, Cartesian tensor notation [2] has been adopted so that the structure of the equations is still easily recognizable. The governing equations for k and ε are:

$$\rho\frac{Dk}{Dt} = \frac{\partial}{\partial x_j}\left(\frac{\mu_T}{\sigma_k}\frac{\partial k}{\partial x_j}\right) + \mu_T\left(\frac{\partial u_i}{\partial x_j} + \frac{\partial u_j}{\partial x_i}\right)\frac{\partial u_i}{\partial x_j} - \rho\varepsilon, \tag{17}$$

$$\rho\frac{D\varepsilon}{Dt} = \frac{\partial}{\partial x_j}\left(\frac{\mu_T}{\sigma_\varepsilon}\frac{\partial \varepsilon}{\partial x_j}\right) + \frac{C_{\varepsilon 1}\mu_T\varepsilon}{k}\left(\frac{\partial u_i}{\partial x_j} + \frac{\partial u_j}{\partial x_i}\right)\frac{\partial u_i}{\partial x_j} - \frac{\rho C_{\varepsilon 2}\varepsilon^2}{k}, \tag{18}$$

where the left-hand side of (17) and (18) represent transport of k and ε, respectively. The three terms on the right-hand sides of (17) and (18) represent diffusion, production and dissipation, respectively. These two equations are derived from the unsteady Navier–Stokes equations with the introduction of the diffusive

terms, the neglect of terms representing viscous dissipation and the modification of some other terms. From the local values of k and ε, a local (turbulent) eddy viscosity μ_T can be evaluated as [4],

$$\mu_T = \frac{C_\mu \rho k^2}{\varepsilon} \tag{19}$$

and the eddy viscosity is used to relate the Reynolds stresses (e.g. in (13) and (14)), to the mean quantities by

$$-\overline{\rho u_i' u_j'} = \mu_T \left(\frac{\partial u_i}{\partial x_j} + \frac{\partial u_j}{\partial x_i} \right) - \frac{2}{3} \rho k \delta_{ij}. \tag{20}$$

In Eqs. (17)–(19) the following values are used for the empirical constants [2,5]:

$$C_\mu = 0.09, \quad C_{\varepsilon 1} = 1.45, \quad C_{\varepsilon 2} = 1.90, \quad \sigma_k = 1.0, \quad \sigma_\varepsilon = 1.3. \tag{21}$$

The use of (17) and (18) implies that $\mu_T \gg \mu$. This is clearly invalid close to a solid wall where the turbulent fluctuations are suppressed by the presence of the wall. Therefore, adjacent to walls special wall functions are introduced [7,9] that typically assume a logarithmic dependence of the tangential velocity component on the normal coordinate and that the production of turbulent kinetic energy is equal to the dissipation in the log-law region. This is equivalent, in the simplest form, to introduce a mixing-length eddy viscosity formulation adjacent to a wall. The use of the special wall functions provide boundary conditions on k and ε away from the wall. Alternatively, additional terms [7] are added to (17) and (18) and boundary conditions $k = 0$, $\partial\varepsilon/\partial n = 0$ are applied at the wall.

The k–ε turbulence model is suitable for computing free shear layers, boundary layers, duct flows and separated flows; although predictions of far-wake unconfined separated flows overestimate the turbulence production [4]. The major weakness of the k–ε model is the assumption of an isotropic eddy viscosity (20). This can be avoided by introducing a separate partial differential equation for each Reynolds stress. However, this increases the computational cost substantially. An effective intermediate model assumes that the transport of the individual Reynolds stresses is proportional to the transport of k. This reduces the differential equations for the Reynolds stresses to algebraic equations. The details of the algebraic stress model and turbulence models are provided [2].

4. Analysis of the results

It is possible to note the followings points based on the obtained results

- From the suction on the upper face of the roof point of view, it is accepted that the most unfavorable case for the roof is in case of lateral stream. When the direction of the stream is longitudinal or oblique the zones of suction are considerably smaller.
- As it was said previously, the pitot tubes project 5 mm with respect to the surface. This means that the values of C_P measured are not exactly on the roof, but at a height of 5 mm above the same. Taking into account that the scale of the model is 1:100, this pressure distribution would belong to the prototype but at 0.5 m of height on the roof.

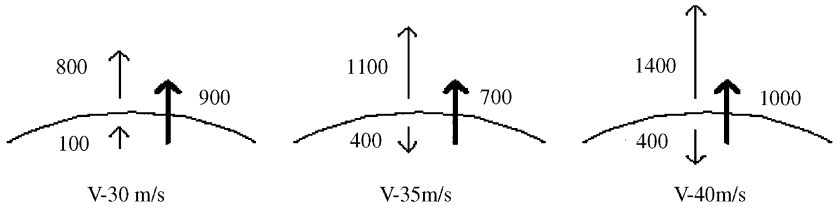

Fig. 3. Calculation of the net pressure on the roof.

- Asymmetries are observed in the C_P values obtained in cases of lateral and longitudinal streams. These mistakes may be the result of stream perturbations, errors in the measurement devices, bad position of the model with respect to the stream or lack of geometrical symmetry of the model.
- The pressure distributions in the lower face of the roof have not been measured. Perhaps because it was assumed that there were no important variations of pressure on the lower face.

Since the case of transverse wind stream is the most unfavorable, by means of the finite element method only this case will be studied. It is also checked if it is necessary to take into account the pressure variations taking place in the lower face of the roof.

From the C_P distribution the dimensionless coefficients of sustentation C_L and resistance C_D can be calculated. Then such calculation is developed in case 1 (simple roof with transverse stream). The measures obtained in the central measurement sections are fitted resulting in the following mathematical expression:

$$C_P = -0.5 \sin\left(4\left(\theta + \frac{\pi}{6}\right)\right) - 0.6, \tag{22}$$

where θ is the position angle in polar coordinates, varying from $-30°$ in the inlet edge to $+30°$ in the outlet edge.

4.1. Results of the bidimensional finite element model

The bidimensional model has been solved with a reference velocity equal to the three-dimensional case, of $V = 30\,\mathrm{m/s}$. Afterwards, the same model has been solved with other velocities to study the influence of this variable. Specifically, it was solved for the velocities $V = 30$, 35, and 40 m/s.

The pressure drop in the upper face of the roof was as high as the velocity of the wind. The same occurs on the lower face of the roof. Therefore, in order to determine the total force on the roof it is necessary to take into account the pressure drop in both faces, as it is shown in Fig. 3.

For a wind velocity of $V = 30\,\mathrm{m/s}$ there is a suction of 800 Pa on the upper face and pressure on the lower face is 100 Pa, so that the net pressure is a suction of 900 Pa.

In case of a higher wind velocity, $V = 35\,\mathrm{m/s}$, a suction on the upper face of 1100 Pa and a suction on the lower face of 400 Pa are obtained. Thus the net pressure will be 700 Pa, increasing.

For a wind stream velocity of $V = 40\,\mathrm{m/s}$, a suction of 1400 Pa in the upper face and a suction of 400 Pa in the lower face are obtained. The net pressure will be 1000 Pa.

In Fig. 4, the numerical results for the velocity and pressure contour lines are shown for the three velocities indicated above.

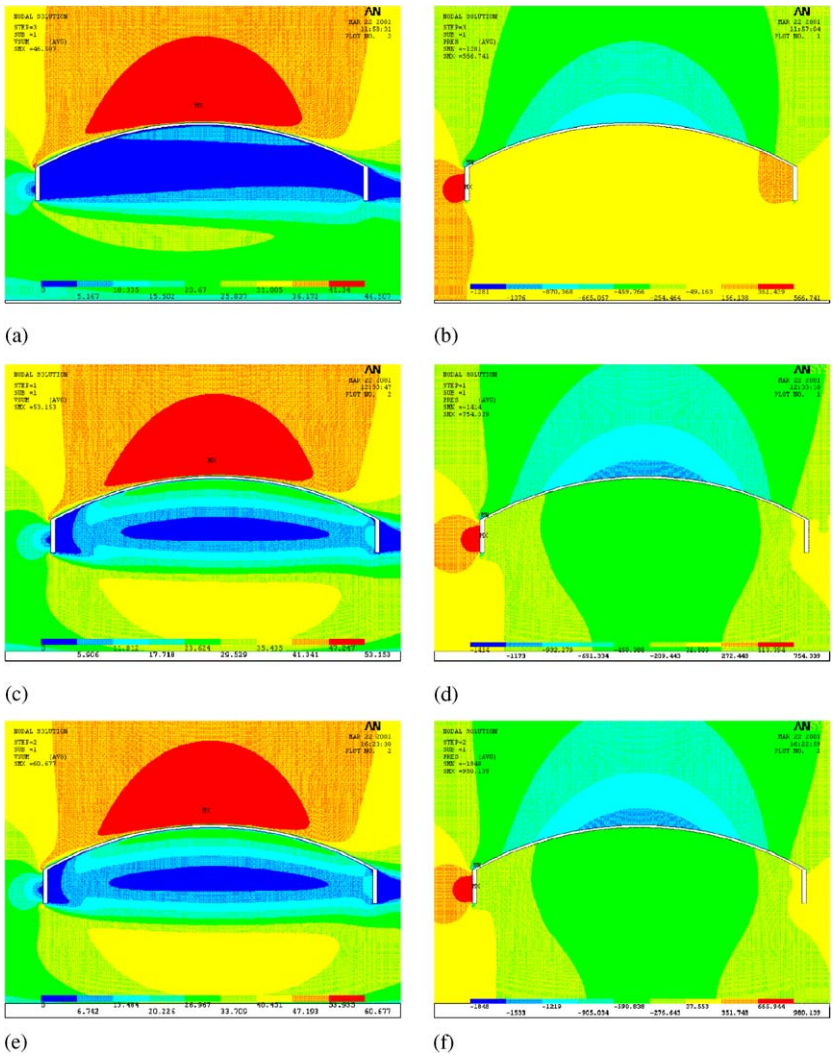

Fig. 4. Numerical results on the roof: (a) velocity contour lines ($V = 30\,\mathrm{m/s}$); (b) pressure contour lines ($V = 30\,\mathrm{m/s}$); (c) velocity contour lines ($V = 35\,\mathrm{m/s}$); (d) pressure contour lines ($V = 35\,\mathrm{m/s}$); (e) velocity contour lines ($V = 40\,\mathrm{m/s}$); and (f) pressure contour lines ($V = 40\,\mathrm{m/s}$).

Comparing the coefficients of pressure estimated by the Standard NBE-AE rule and by the European Standard rule with those obtained by the finite element method (FEM), Fig. 5 is obtained.

As it is noted, the Standard NBE-AE is the only one that considers the case of curved roof and open nave, and therefore it is approximated more to the reality. The European Standard only considers flat roofs when the nave is open. This Standard increases the suction in the ridge and the ends of roof to avoid the separation of stream in these zones.

Due to the huge quantity of constructive possibilities, it is very difficult to elaborate an entire Standard about this subject. Anyway, the finite element method (FEM) [6,10] is shown as an useful and cheap tool to study this phenomenon.

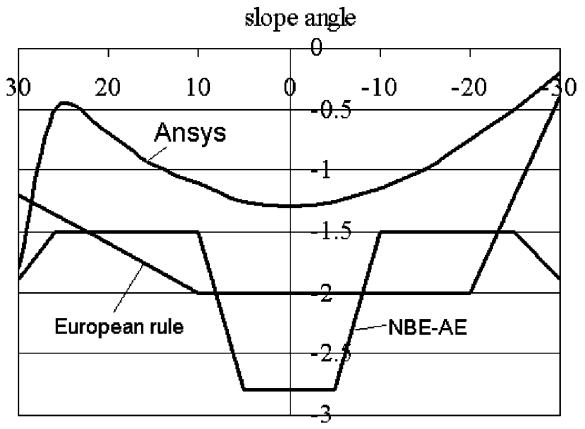

Fig. 5. Coefficients C_P obtained with ANSYS and the estimated one by the Standard rules.

5. Summary and conclusions

A computational procedure has been developed based on the general-purpose finite element code ANSYS-FLOTRAN, for modeling and simulating the air pressure on the self-weighted metallic roofs due to the wind effect. Finite element method along with data from experimental tests carried out in a wind tunnel [8] involving a reduced scale model of a roof are used for comparison purposes. The findings of this study suggest that it may be possible to devise a practical procedure for stabilizing a self-weighted metallic roof model by using a combined experimental/computational approach.

From the experimental measurements it is derived that the suction on the upper face of the roof is the most unfavorable case in case of lateral stream. When the direction of the stream is longitudinal or oblique the zones of suction are considerably small. In case of two roofs the effects of the wind on the second roof are smaller than the first roof.

Acknowledgements

The authors express deep gratitude to Department of Construction and Department of Mathematics at Oviedo University for useful assistance. Helpful comments and discussion are gratefully acknowledged. Our thanks to Swanson Analysis Inc. for the use of University High license of ANSYS program [6].

References

[1] K. Bathe, Finite Element Procedures, Prentice-Hall, Englewood Cliffs, New York, 1996.
[2] C.A.J. Fletcher, Computational Techniques for Fluid Dynamics, Springer, Berlin, 1991.
[3] V. Girault, P.R. Raviart, Finite Element Methods for Navier–Stokes Equations: Theory and Algorithms, Springer, New York, 1986.
[4] C. Hirsch, Numerical Computation of Internal and External Flows, Wiley, New York, 1997.
[5] L.D. Landau, E.M. Lifshitz, Fluid Mechanics, Pergamon Press, New York, 1991.
[6] S. Moaveny, Finite Element Analysis: Theory and Application with Ansys, Prentice-Hall, Englewood Cliffs, New York, 1999.

[7] V.C. Patel, W. Rodi, G. Scheurer, Turbulence models for near-wall and low-Reynolds number flows: a review, AIAA J. 23 (1985) 1308–1319.
[8] Technical Report of the Laboratory of Aerodynamic Buildings, Bundesversuchs und Forschungsanstalt, Arsenal (Vienna-Austria), 2000.
[9] E.R. Van Driest, On turbulent flow near a wall, J. Aerosol Sci. 23 (1986) 1007–1111.
[10] O.C. Zienkiewicz, R.L. Taylor, The Finite Element Method: Solid and Fluid Mechanics and Non-linearity, McGraw-Hill Book Company, London, 1991.